

NUMERICAL INVESTIGATION OF CONJUGATE HEAT TRANSFER PROBLEMS

P. Manna* and Debasis Chakraborty*

Abstract

Conjugate heat transfer (CHT) analysis has been carried out for laminar flow past flat plate and turbulent flow between parallel plates using a commercial CFD software CFX-TASCFlow. Navier-Stokes equations alongwith $k-\epsilon$ turbulence model in the fluid and conduction equation in the solid have been solved simultaneously to obtain the flow features. The computed temperature distribution of the flow past flat plate matches very well with analytical and other numerical results. For the turbulent flow between parallel plates, nondimensional temperature distribution and Nusselt number distribution matches very well with the analytical and experimental results for different values of Reynolds number and thickness of the heat transfer plate.

Introduction

In certain critical applications where working temperature is very high, it is necessary to calculate the temperature distribution in the solid to ensure that it should not cross the metallurgical limit. The Selection of the material and wall thickness is largely dependant on the wall temperature distribution in the solid. Hence, it is necessary to solve the energy equation of the solid alongwith the fluid flow equations, commonly known as conjugate heat transfer problem. This type of problem differs from commonly encountered heat conduction problems, as the temperature of the fluid which is used to cool (or heat) the solid is not known a priori. Instead, the fluid temperature is calculated at the same time as the solid temperature. In most of the earlier works, the temperature distribution in the boundary layer of the main stream is determined under a prescribed condition at the surface and then the heat transfer coefficient is calculated. Next the heat transfer process in the solid is calculated. Thus, the complexity of the heat transfer processes between the fluid and the main stream is described by a pre-determined heat transfer coefficient which shows heat transfer process is independent of the solid properties. Contrary, the recent works of the convective heat transfer problems with conjugate heat transfer seems to be more physical compared to the earlier works as the calculations for the fluid and the solid are done simultaneously.

The works reported in the field of conjugate heat transfer are mostly analytical. Few experimental studies are made for laminar and turbulent flow. Numerical stud-

ies are relatively scarce. The geometries taken into consideration are flow over flat plate, flow between heated parallel plates or rectangular ducts, surface mounted heat blocks in forced or natural flow, finned-tube in cross flow, circular cylinders in uniform flow etc. Luikov [1] has derived two approximate engineering solutions of conjugate heat transfer problem based on local Nusselt number for a laminar incompressible flow around a flat plate of finite thickness for Prandtl number near or less than unity. One is based on a differential analysis assuming a uniform velocity profile in the thermal boundary layer and the other is an integral analysis based on polynomial representations of velocity and temperature profiles. Incompressible flow past flat plate has also been studied by Payvar [2] obtained useful solutions for higher Prandtl numbers also. Adami et.al [3] upgraded a finite volume CFD solution for conjugate heat transfer analysis. The upgraded solution was validated against theoretical results [1] on simple flow over a flat plate and film-cooled plate before applying a complex flow problem on 3-D film cooled turbine blade.

Davis and Gill [4] have studied the effect of wall conduction on flow between parallel plates for laminar flow while the turbulent flow effects are studied by Sakakibara and Endoh [5]. Analytical solutions are worked out to predict the experimental observations of the axial conduction in the wall. They have shown that the Prandtl number, Reynolds number, ratio of conductivity of the solid wall to that of the fluid, thickness to length ratio of the wall are the important parameters to determine the effect of the wall conduction.

* Scientist, Computational Combustion Dynamics Division, Directorate of Computational Dynamics, Defence Research and Development Laboratory, Kanchanbagh Post, Hyderabad - 500 058, India, Email : debasis_ccd@drdl.ernet.in

The numerical simulation of conjugate heat transfer analysis has not been reported adequately in the literature. Kasagi et al. [6] developed a numerical model for two dimensional channel flow alongwith unsteady heat conduction by incorporating three fluctuating velocities into the governing equations obtained from Streamwise pseudo-Vortical Motion (SPVM) model. It was observed that the near-wall behaviour of temperature variance, turbulent heat flux and turbulent Prandtl number is strongly influenced by the thermal properties and thickness of the wall and the coherent turbulent structures also play an important role in the scalar transport process near the wall. Direct Numerical Simulation (DNS) [7] was also applied to the conjugate heat transfer problem for a fully developed two dimensional channel flow. Various statistical quantities of thermal field were analysed and compared with the numerical results with the studies of Kasagi et al [6]. The DNS study confirmed most of the Kasagi's conclusions. It was concluded that the role of DNS is largely confined in determination of various parameters in the simpler models.

Conjugate heat transfer from surface mounted block(s) to forced convection air flow in a parallel plate channel was modeled by Nakayama and Park [8] and the accuracy of the numerical prediction of the thermal conductance for different heat flow paths was proven experimentally. An array of heated square blocks deployed along one wall of parallel-plate channel was simulated [9] and detailed parametric studies were presented for various Reynolds number and various of geometric and heated area parameters. The conjugate heat transfer problem for a circular cylinder with a heated core region in low Reynolds number flow has been studied numerically by Suden [10]. The ratio of solid and fluid thermal conductivity (k_s/k_f) has been found to greatly influence the heat transfer.

In the present work, the commercial software, CFX-TASCFlow [11] is used to solve the fluid flow equations and the heat conduction equation in the solid simultaneously. The code has been validated for a laminar flow past a flat plate problem [1 and 3] and the computed temperature distribution are compared with other numerical and analytical results. The software was then applied to the turbulent flow past between two parallel plates which is having a very good practical application in the design of heat exchangers as it is desirable to use short passages with turbulent flow in a heat exchanger in order to take advantages of the high heat transfer coefficients in the entrance region. The computed temperature and heat transfer coef-

ficient distribution are compared with the experimental [5] and other analytical [5] results.

Methodology

The computational domain of a CHT problem consists of the fluid domain and solid domain. In fluid domain, the three dimensional Navier-Stokes equations are solved for velocity components, pressure, density, temperature etc. In the CHT solid, diffusion is the only transport process, and only the energy equation is solved for temperature. The fluid energy and the solid energy equations are coupled for the identical conditions of temperature and heat flux at the solid-fluid interface. The governing equations in fluid and solid are solved using the 3-D Navier-Stokes Code-CFX TASCFlow which is an integrated software system capable of solving diverse and complex multidimensional fluid flow problems. The code is fully implicit, finite volume method with finite element based discretisation of geometry. It utilizes numerical upward schemes to ensure global convergence of mass, momentum and energy. It implements a general non-orthogonal, structured, body fitted grids. In the present study, the discretisation of the convective terms are done by first order upwind difference scheme. The turbulence model used was $k - \epsilon$ model with wall functions.

Basis Theory

For the **fluid domain**, the conservation of mass is

$$\frac{\partial \rho}{\partial t} + \frac{\partial}{\partial x_j} (\rho u_j) = 0 \quad j = 1, 2, 3 \quad (1)$$

The conservation of momentum equation is

$$\frac{\partial}{\partial t} (\rho u_i) + \frac{\partial}{\partial x_k} (\rho u_i u_k) = - \frac{\partial p}{\partial x_i} = \frac{\partial}{\partial x_i} \left(\mu_{eff} \left(\frac{\partial u_i}{\partial x_k} + \frac{\partial u_i}{\partial x_i} \right) - \frac{2}{3} \mu_{eff} \frac{\partial u_l}{\partial x_l} \delta_{ij} \right) \quad i, k = 1, 2, 3 \quad (2)$$

The total energy equation is

$$\frac{\partial}{\partial t} (\rho H) - \frac{\partial p}{\partial t} + \frac{\partial}{\partial x_j} (\rho u_j H) = \left(q_j + \frac{\mu_t}{Pr_t} \frac{\partial h}{\partial x_j} \right) + \frac{\partial}{\partial x_j} \left\{ u_i \left[\mu_{eff} \left(\frac{\partial u_i}{\partial x_k} + \frac{\partial u_i}{\partial x_i} \right) - \frac{2}{3} \mu_{eff} \frac{\partial u_l}{\partial x_l} \delta_{ij} \right] + \mu \frac{\partial k}{\partial x_j} \right\} \quad (3)$$

Turbulent kinetic energy (k) equation:

$$\frac{\partial}{\partial t} (\rho k) + \frac{\partial}{\partial x_k} (\rho u_k k) = \frac{\partial}{\partial x_k} \left(\left(\frac{\mu_l}{Pr} + \frac{\mu_t}{\sigma_k} \right) \frac{\partial k}{\partial x_k} \right) + S_k \quad (4)$$

Rate of dissipation of turbulent kinetic energy (ϵ) equation :

$$\frac{\partial}{\partial t} (\rho \epsilon) + \frac{\partial}{\partial x_k} (\rho u_k \epsilon) = \frac{\partial}{\partial x_k} \left(\left(\frac{\mu_l}{Pr} + \frac{\mu_t}{\sigma_\epsilon} \right) \frac{\partial \epsilon}{\partial x_k} \right) + S_\epsilon \quad (5)$$

where, ρ , u_i , p , $H (= h + 0.5 u_i u_i + k)$ are the density, velocity components, pressure and total energy respectively and $\mu_{eff} = \mu_l + \mu_t$ is the total viscosity; μ_l , μ_t being the laminar and turbulent viscosity and Pr is the Prandtl number. The source term S_k and S_ϵ of the k and ϵ equation are defined as

$$S_k = \tau_{ik} \frac{\partial u_i}{\partial x_k} - \rho \epsilon \quad \text{and} \quad S_\epsilon = C_{\epsilon 1} \tau_{ik} \frac{\partial u_i}{\partial x_k} - C_{\epsilon 2} \frac{\rho \epsilon^2}{k}$$

where turbulent shear stress is defined as

$$\tau_{ik} = \mu_t \left(\frac{\partial u_i}{\partial x_k} + \frac{\partial u_k}{\partial x_i} \right)$$

Laminar viscosity (μ_l) is calculated from Sutherland law as

$$\mu_l = \mu_{ref} \left(\frac{T}{T_{ref}} \right)^{3/2} \left(\frac{T_{ref} + S}{T + S} \right)$$

where, T is the temperature and μ_{ref} , T_{ref} and S are known coefficient. The turbulent viscosity μ_t is calculated as

$$\mu_t = c_\mu \frac{\rho k^2}{\epsilon}$$

The coefficients involving in the calculation of μ_t are taken as

$$\begin{aligned} c_\mu &= 0.09, & C_{\epsilon 1} &= 1.44, & C_{\epsilon 2} &= 1.92 \\ \sigma_k &= 1.0, & \sigma_\epsilon &= 1.3, & \epsilon_c &= 0.9 \end{aligned}$$

The heat flux q_j is calculated as $q_j = -\lambda_f \frac{\partial T}{\partial x_j}$, λ_f is the thermal conductivity of fluid.

In the **CHT solid**, diffusion is the only transport process, and the energy equation reduces to

$$\frac{\partial}{\partial t} (\rho c T) = \frac{\partial}{\partial x_j} \left(\lambda_s \frac{\partial T}{\partial x_j} \right) \quad (6)$$

where, c is specified heat and λ_s is the thermal conductivity of the solid.

A special condition is applied between the fluid energy and the solid energy equation everywhere the fluid boundary face and a CHT solid boundary face are coincident. This CHT interface condition allows energy to flow between the fluid and the solid.

The CHT interface condition is implemented in the fluid and solid energy equation as follows :

$$q_f = q = -\lambda_f \frac{\partial T}{\partial y} = -\lambda_f \frac{T - T_f}{\Delta y_f} \quad (7)$$

where, λ_s = fluid conductivity, T = the interface temperature and T_f = adjoining fluid temperature

$$q_s = q = -\lambda_s \frac{\partial T}{\partial y} = -\lambda_s \frac{T - T_s}{\Delta y_s} \quad (8)$$

where, λ_s = solid conductivity, and T_s = adjoining solid temperature

Combining equation (7) and (8) yields,

$$q = \frac{T_f - T_s}{\frac{\Delta y_f}{\lambda_f} + \frac{\Delta y_s}{\lambda_s}} \quad (9)$$

This is the final expression for the heat flux which is incorporated in place of $\lambda \frac{\partial T}{\partial y}$ both in fluid and solid energy equation at the interface. And the interface temperature is calculated as,

$$T = T_f + \frac{T_f - T_s}{\frac{\Delta y_f}{\lambda_f} + \frac{\Delta y_s}{\lambda_s}} \frac{\Delta y_f}{\lambda_f} \quad (10)$$

The CHT interface boundary temperature and the heat flux are calculated implicitly in the simulation.

Results and Discussion

Two cases have been considered for the analysis of conjugate heat transfer problems. The first one is laminar flow over a flat plate with conjugate heat transfer between the gas and the plate and the second one is conjugate heat transfer in a turbulent flow between parallel plates.

Conjugate Heat Transfer in Laminar Flow Over a Flat Plate

Luikov [1] has derived the analytical solution for laminar flow over a flat plate with conjugate heat transfer between the fluid and the solid. The total temperature of air is taken as 1400 K with a Mach number of 0.13 which corresponds to an inlet velocity of 94.9 m/s. The conjugate heat transfer plate has a thickness of 10 mm with thermal conductivity of 4.0 W/m-K. The plate is cooled from the below. The wall of the cooling surface is maintained at 600 K. The velocity profile is taken as flat at inlet of the test section. Adami et.al [3] numerically simulated flow over a flat plate for hot air flow with conjugate heat transfer between the gas and the plate and compared their numerical results with the analytical solution of Luikov [1] with reasonable agreement. This test case is taken as the first case for validation. The test section length (L) is 200 mm. The Reynolds number of the flow calculated based on $L=200$ mm is about 1.1×10^5 which ensures the flow of the entire computational domain is laminar. Total height of the test section is 100 mm, which is sufficiently large to ensure no effect of the boundary layer reaches at the top boundary of the domain. The geometry of the computational domain is shown in Fig.1. The X -axis is taken along the flow while the Y direction is considered normal to the flow. The fluid-solid interface at inlet is taken as the reference of the X and Y -axis. The grid structure of the computational domain is shown in Fig.2. A non-uniform structured grid of $186 \times 131 \times 3$ is used in the simulation. As the problem is treated as two dimensional, only 3 grid points are taken in the Z -direction. The grids are very fine at inlet and CHT solid-fluid interface, typically, with minimum spacing of 0.05 mm in the Y -direction. The grid independence of the results is demonstrated by comparing the temperature profile at $X = 50$ mm

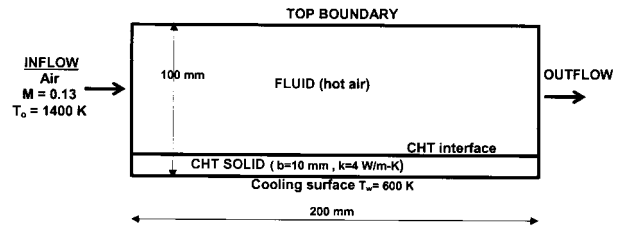


Fig. 1 Schematic of the computational domain



Fig. 2 Grid structure of the computational domain
($186 \times 131 \times 3$)

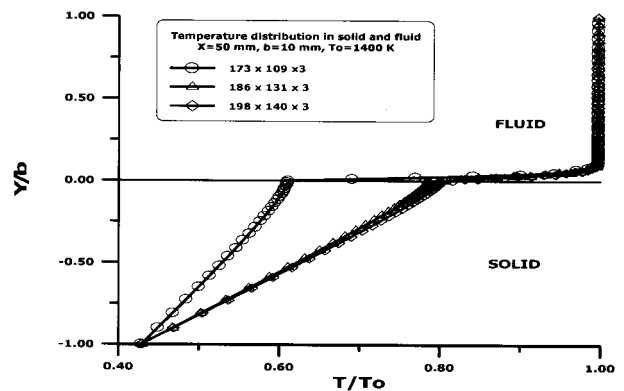


Fig. 3 Temperature distribution in solid and fluid at $X=50$ mm

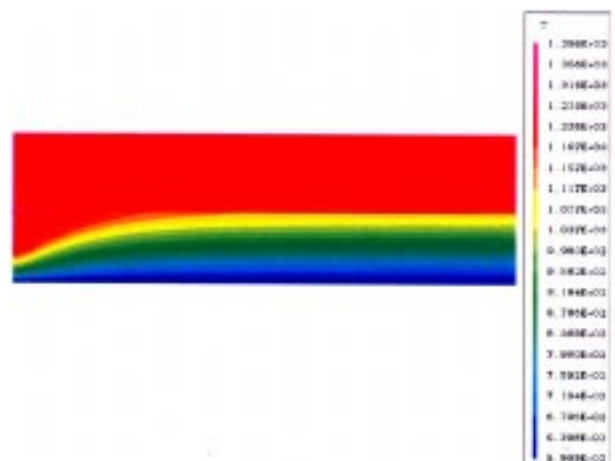


Fig. 4 Temperature distribution in the computational domain

with three different grids, namely 173 x 109 x 3, 186 x 131 x 3 and 198 x 140 x 3. It is clear from Fig.3, that by changing the grid structure from 186 x 131 x 3 to 198 x 140 x 3, the results almost remain unchanged. The qualitative feature of the temperature field is shown in Fig.4 where the blown-up view of the solid-fluid interface has been presented. The temperature change occurs almost uniformly along the normal direction in the solid but in the fluid, the temperature is changed primarily adjacent to the boundary layer. The interface temperature rapidly falls along the flow direction upto about four plate thickness distance, and then almost remains constant downstream of the flow (Fig.5). The non-dimensionalised temperature profile (T/T_o) along the normal direction from interface in two axial locations, namely, at $X = 10$ and 80 mm are compared with the analytical solution of Luikov [1] and numerical solution of Adami et.al [3] in Figs.6 and 7 respectively. The present computational results match well with both analytical and other numerical results. The boundary layer resolution for the present computation is better compared to the numerical solution of Adami et.al. To see the effect of conjugate heat transfer analysis on the flow field, two different simulations have been done excluding CHT analysis where the boundary of the fluid at interface is maintained at 600 K for the 1st case and adiabatic condition for the other case. The results of the velocity and temperature profiles for both the simulation have been compared at two axial locations, $X = 10$ and 80 mm in Figs.8 and 9 respectively. Though, there is marginal difference in axial velocity distribution, large differences in temperature distribution have been observed for all the cases, particularly in the interface region. The isothermal wall boundary condition gives the minimum temperature distribution (600 K at interface) whereas the adiabatic wall boundary condition shows the maximum temperature distribution (1396.1 K at interface) on the interface and the boundary layer. The results with conjugate heat transfer in solid show a temperature distribution (1211 K and 1093 K at interface for $X = 10$ and 80 mm respectively) somewhat in between the two which can be considered as the most practical solution for the design purposes.

Conjugate Heat Transfer with Turbulent Flow between Parallel Plates

Sakakibara and Endoh [5] have done an experimental investigation to measure the local temperature and heat transfer coefficient for a turbulent flow fully developed in a rectangular duct consisting of a 200 cm length, 15 cm wide and 3 cm high. A 30 cm heat transfer plate of hard polyvinyl Chloride (PVC) extending the width of the

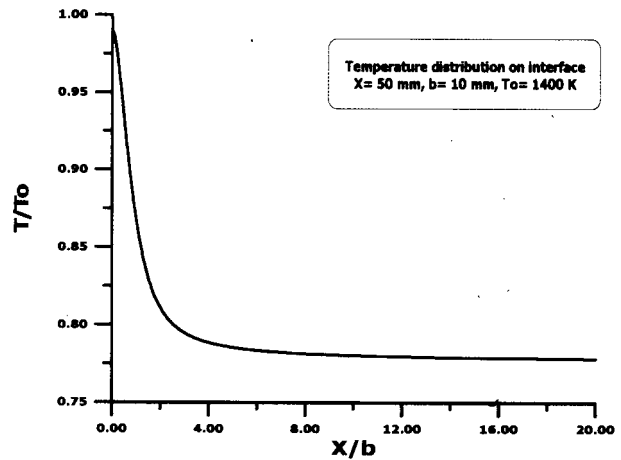


Fig. 5 Temperature distribution at interface

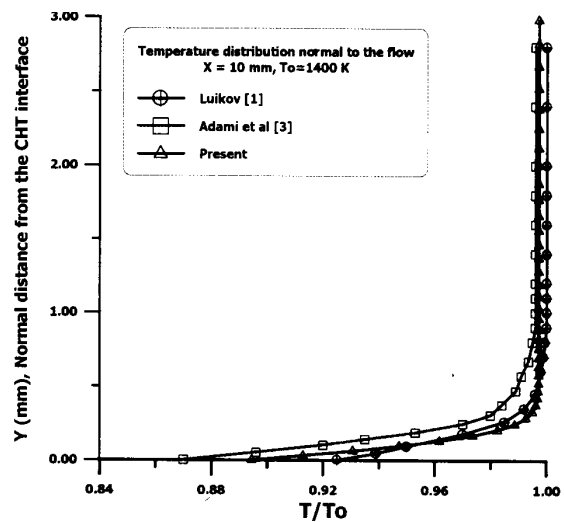


Fig. 6 Temperature distribution at X = 10 mm

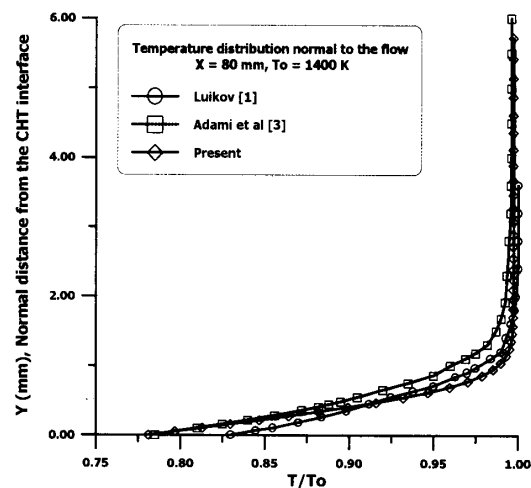
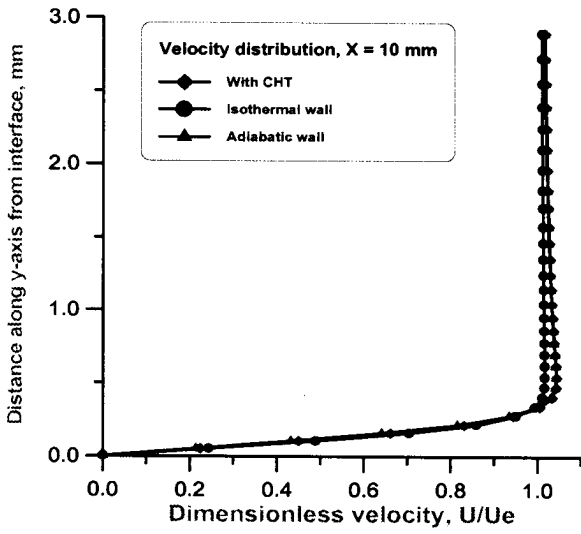
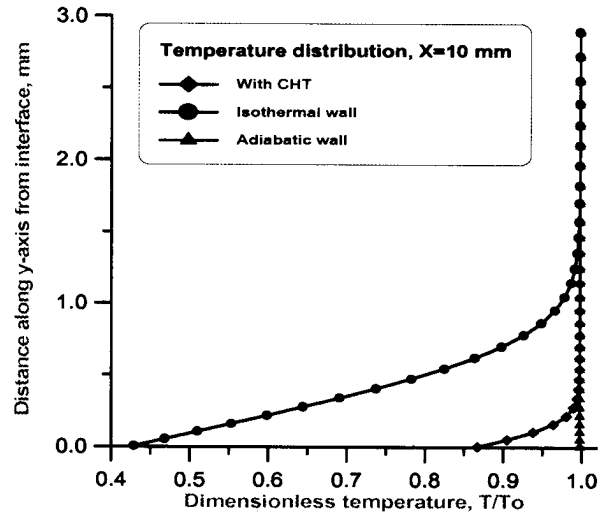


Fig. 7 Temperature distribution at X = 80 mm

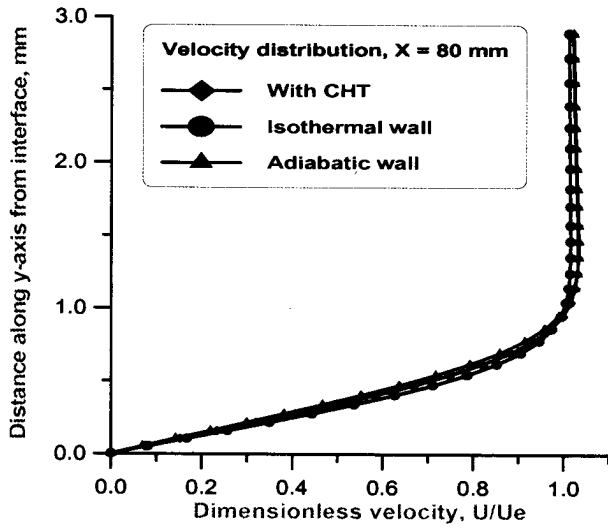


(a)

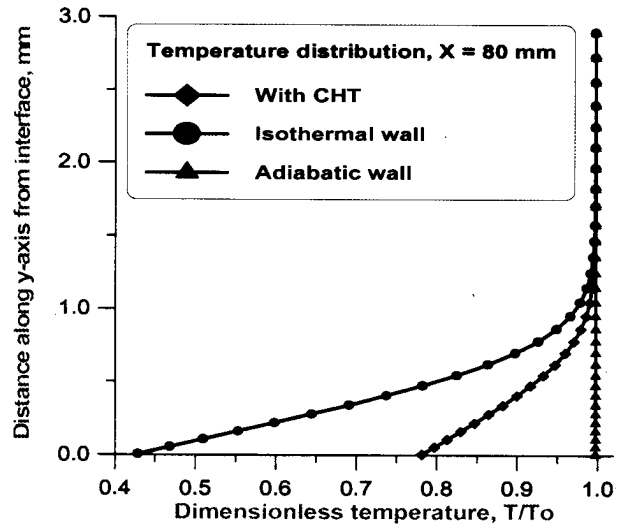


(b)

Fig. 8 Comparison of results at X = 10 mm (a) Axial velocity (b) Temperature



(a)



(b)

Fig. 9 Comparison of results at X = 80 mm (a) Axial velocity (b) Temperature

Table-1 : Test Conditions for the Computations						
Test Run No.	Inlet Velocity, U_o (m/s)	Inlet Temp. T_e (K)	Length of the Heat Transfer Plate, L (m)	Height of the Fluid Domain, H/L	Height of the Solid Domain, b/L	Re, $(2U_oH/\nu)$
1.	6.8	290.3	0.3	0.1	0.038	27813
2.	6.1	290.3	0.3	0.1	0.069	24665
3.	6.1	290.3	0.3	0.1	0.1033	24665

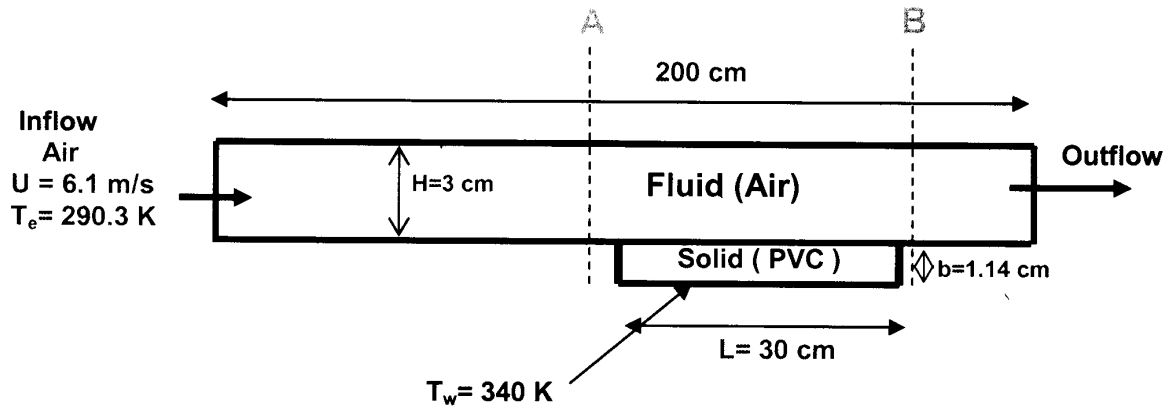


Fig. 10 Schematic of the computational domain (not to scale)

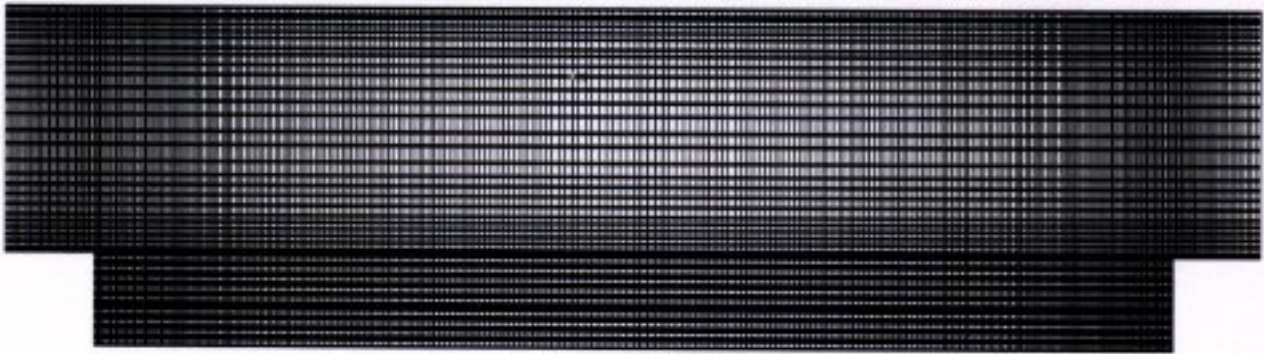


Fig. 11 Grid structure of the computational domain, $749 \times 46 \times 3$ (A-B)

duct was installed 150 cm from the inlet. A heating chamber was installed at the bottom of the heat transfer plate to maintain a constant temperature at the bottom surface of the plate. The entire test section was insulated to minimize the heat losses. To get the interfacial temperature and the local heat transfer coefficient, five thermocouples were installed in five locations at interface and other five within the solid, perpendicular to the flow. From the measured temperature distribution, the interfacial temperature and local heat flux was estimated and the local Nusselt number was calculated. From the data of velocity, it was confirmed that the horizontal velocity distribution of the duct was almost uniform within the 10 cm wide and hence, the problem is taken as two-dimensional for their analytical solution. The schematic diagram of the test set-up is shown in Fig. 10. The geometry and the test conditions are taken identical to the experiment as explained above. The X axis is taken along the flow direction and Y direction is normal to the flow direction. The origin of the X and Y axis is taken at the starting of the solid-fluid interface, i.e. 150 cm apart from the inlet of airflow. A large length of the fluid flow domain ahead of heat transfer plate is taken to

get a fully developed flow between the parallel plates as the flow approaches close to the heat transfer plate. The grid structure of the computational domain (between A and B as marked in Fig. 10) is shown in Fig. 11. A non-uniform structured grid of $749 \times 46 \times 3$ is used for the simulation. Very fine grids are provided near the wall, in heat transfer plate, at interface region and the locations adjacent to both ends of the plate. The computations are carried out for two Reynolds numbers and three different values of thicknesses of the heat transfer plate. The inflow parameters for computation and geometric details are presented in Table-1.

The grid independence of the results is demonstrated comparing the temperature profile at $X = 50$ mm (for $b/L = 0.038$) with two different grids in Fig. 12. No change in results is observed by changing the grids from $749 \times 46 \times 3$ to $852 \times 61 \times 3$. The axial velocity distribution at $X = 0.0$ mm i.e. the place at which the flow approaches the CHT interface, is shown in Fig. 13 for $Re = 24,665$, $b/L = 0.037$. The computing velocity profile agrees well with the experimental results. The axial distribution of the

non-dimensionalised temperature (T^*) is compared with experimental and the analytical results [5] for three different heights of the solid domain, namely $b/L = 0.037, 0.069$ and 0.1033 in Figs. 14(a), (b) and (c) respectively. The axial distance is normalized with L , the length of the solid (PVC) and the non-dimensionalised temperature is defined as $T^* = (T_s - T_w)/(T_e - T_w)$, where T_s, T_e and T_w are solid-fluid interface temperature, the inlet air temperature and the wall temperature at the bottom surface of the plate, respectively. The computational results show very good comparison with the experimental and analytical [5] results for all the three different height of the solid domain. From these results, it is clear that the interface temperature increases as the thickness of the solid is increased. From

the computed temperature distribution, heat flux $q (= k_s \Delta T/\Delta y)$ between the fluid and the solid and the heat transfer coefficient, $h (= q/(T_s - T_e))$ are calculated. Temperature at the interface and the temperature in the next adjacent gridline within the solid along the Y -axis are used in the calculation. The axial distribution of non-dimensionalised heat transfer coefficient, $Nu (= hD_h/k_f)$ is compared with experimental and analytical [5] results in Figs. 15(a) (b) and (c) for three different heights of solid domain, where D_h is the length scale which is taken as twice the height of the fluid domain and k_f is the fluid conductivity. The present results agree well with the analytical solution and experimental results except $b/L = 0.1033$ where both present results and analytical results slightly under predicted

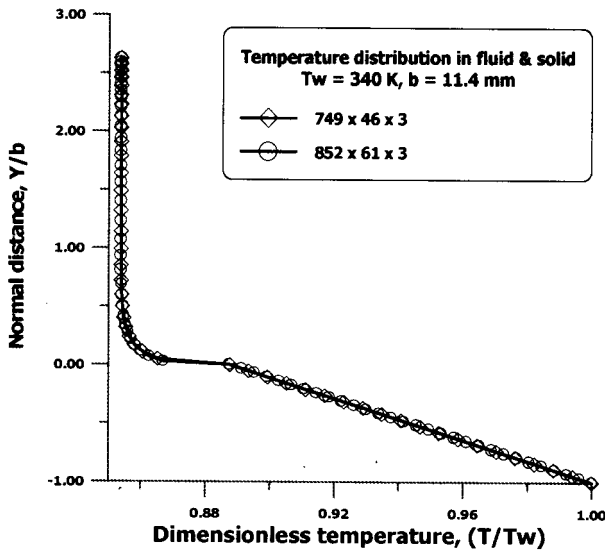


Fig. 12 Temperature distribution for two grids, $X = 50$ mm

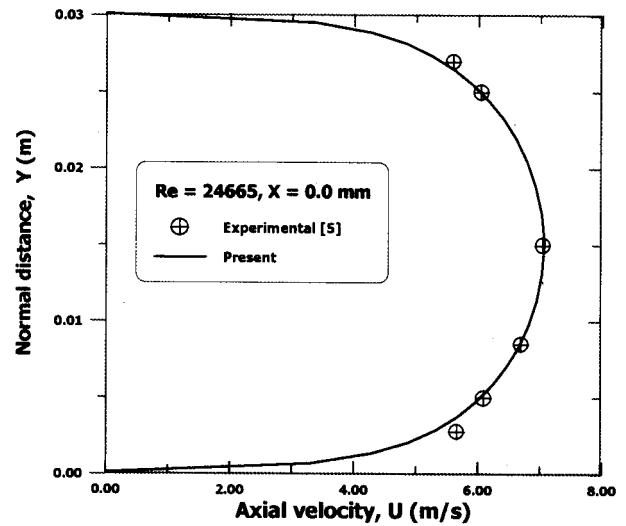


Fig. 13 Velocity profile at starting of interface

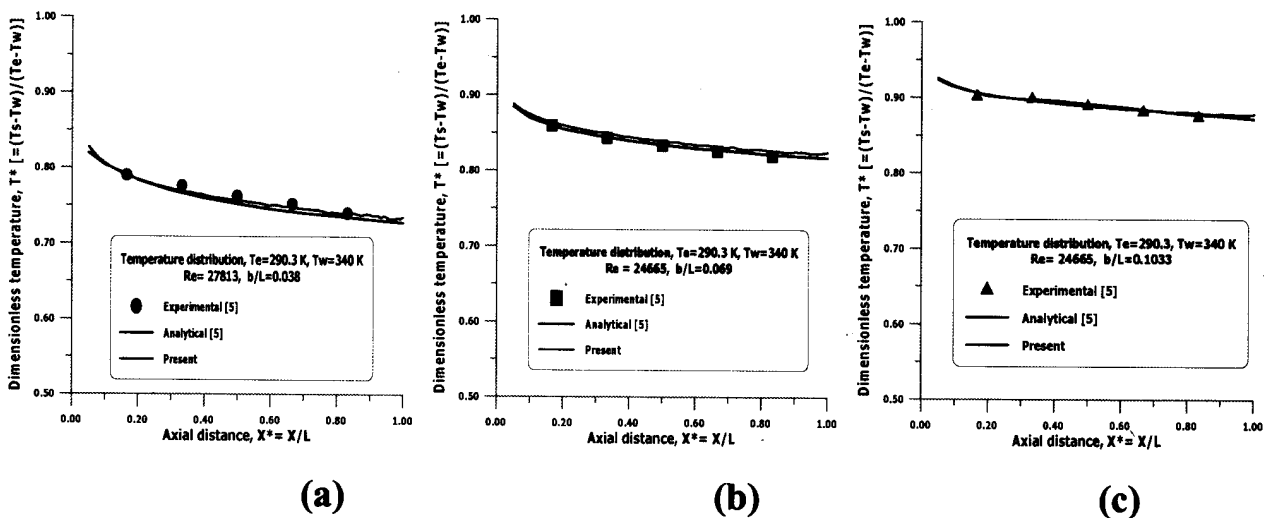


Fig. 14 Temperature profile at interface (a) $b/L = 0.038$ (b) $b/L = 0.069$ (c) $b/L = 0.1033$

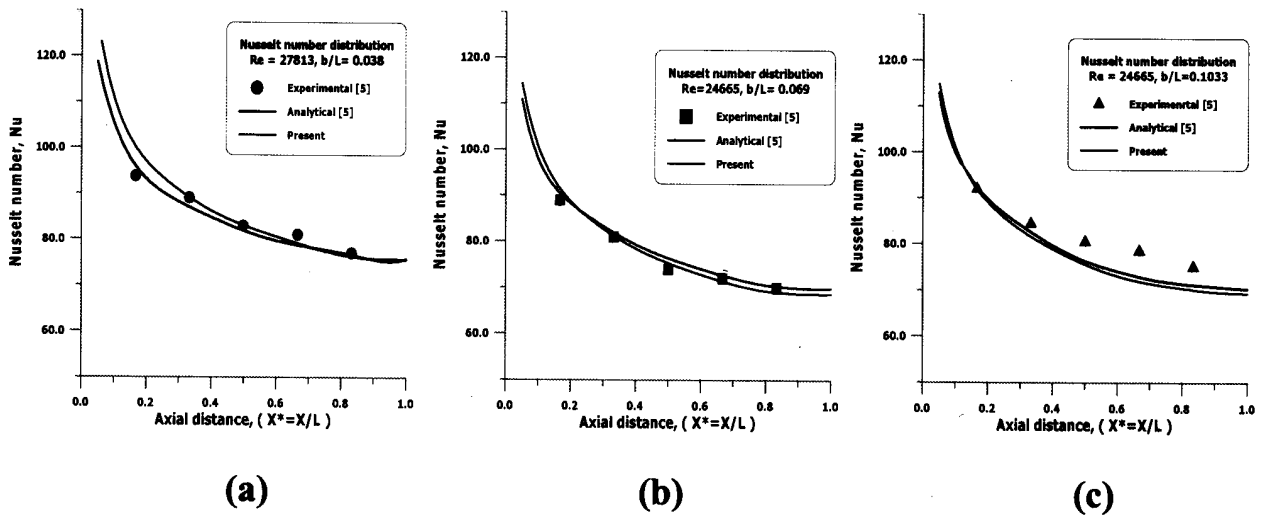


Fig. 15 Nusselt number distribution at interface (a) $b/L = 0.038$ (b) $b/L = 0.069$ (c) $b/L = 0.1033$

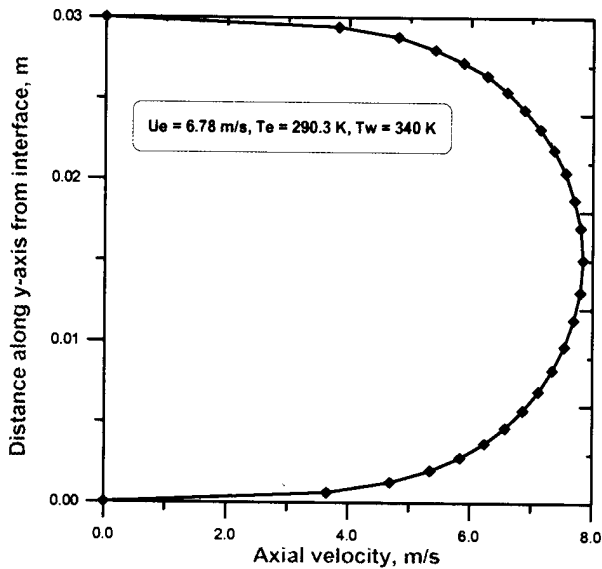


Fig. 16 Axial velocity distribution along the normal direction from interface at $X = 15$ cm

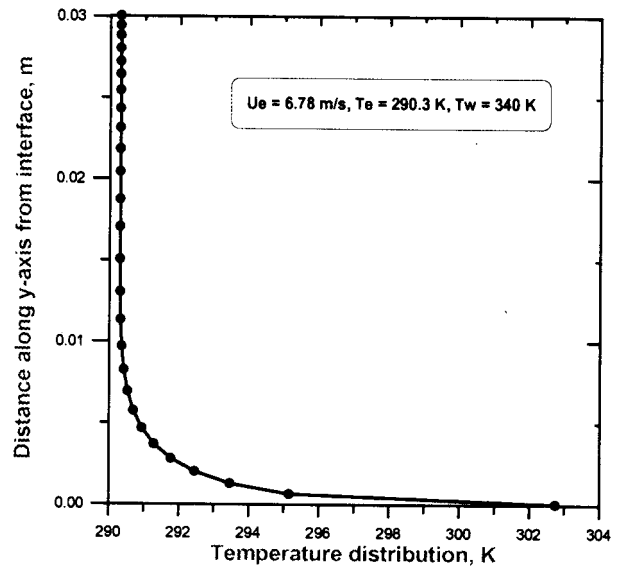


Fig. 17 Temperature distribution along the normal direction from interface

the Nusselt number. In the present simulation the upper plate was maintained at adiabatic condition whereas bottom plate was attached with a CHT solid. The velocity and temperature distributions in the fluid domain at $X = 15$ cm are presented in Figs.16 and 17 respectively to see the effect of wall boundary conditions. Although there is no appreciable change in the velocity profile from its value at the inlet in CHT region, temperature distribution has changed significantly. The temperature of the upper wall which is maintained at adiabatic conditions is almost identical to the inlet temperature whereas the effect of conjugate heat transfer from solid is reflected on the

temperature distribution at bottom surface and the adjacent boundary layer.

Concluding Remarks

The conjugate heat transfer analysis is carried out for both laminar and turbulent flow past a flat plate and the flow between two parallel plates using a commercial CFD software CFX-TASCFlow. The validation case corresponds to CHT problem for the flow past flat plate with $M = 0.13, T_o = 1400$ K. The methodology is applied for turbulent flow past two parallel plates with a heat transfer solid of PVC is placed in the bottom wall to understand

the flow characteristics in heat exchangers. The simulation captures well all the essential features of the flow field. The computed temperature profiles at various axial locations agree very well with analytical and other computational results. The non-dimensional temperature and heat transfer coefficient distribution match with the experimental and analytical solution. The effect of wall boundary conditions on velocity and temperature distribution has been presented considering with/without CHT solid. The good agreement of the computations for the problems gives enough confidence to apply it for the other practical configurations, where high temperature and velocity will be encountered.

References

1. Luikov, A.V., "Conjugate Heat Transfer Problems", *Int. J. Heat Mass Transfer*, Vol.17, 1974, pp.257-265.
2. Payvar, P., "Convective Heat Transfer to Laminar Flow Over a Plate of Finite Thickness", *Int. J. Heat Mass Transfer*, Vol.20, 1977, pp.431-433.
3. Adami, P., Martelli, F. and Montomoli, F., "A Finite Volume Method for the Conjugate Heat Transfer in Film Cooling Devices", *International Symposium of Air-Breathing Engine*, Paper No. ISABE-2003, 1066, September 2003.
4. Davis, E.J.M. and Gill, W.N., "The Effects of Axial Conduction in the Wall on Heat Transfer with Laminar Flow", *Int. J. Heat Mass Transfer*, Vol.13, 1970, pp.459-470.
5. Sakakibara, M. and Endoh, K., "Effect of Conduction in Wall on Heat Transfer with Turbulent between Parallel Plates", *Int. J. Heat Mass Transfer*, Vol.20, 1977, pp.459-470.
6. Kasagi, N., Kuroda, A. and Hirata, M., "Numerical Investigation of Near-Wall Turbulent Heat Transfer Taking into Account the Unsteady Heat Conduction in the Solid Wall", *Journal of Heat Transfer*, Vol.111, 1989, pp.385-392.
7. Tiselj, I., Bergant, R., Mavko, B., Bajcsik, I. and Hetsroni, G., "DNS of Turbulent Heat Transfer in Channel Flow with Heat Conduction in the Solid Wall" *Journal of Heat Transfer*, Vol.123, 2001, pp.849-857.
8. Nakayama, W. and Park, S.H., "Conjugate Heat Transfer from a Single Surface-Mounted Block to Forced Convective Air Flow in a Channel", *Journal of Heat Transfer*, Vol.118, 1996, pp.301-309.
9. Asako, Y. and Faghri, M., "Three-Dimensional Heat Transfer of Arrays of Heated Square Blocks", *Int. J. Heat Mass Transfer*, Vol.32, 1989, pp.395-405.
10. Bengt Suden., "Conjugated Heat Transfer from Circular Cylinders in Low Reynolds Number Flow", *Int. J. Heat Mass Transfer*, Vol.13, 1980, pp.1359-1367.
11. CFX-TASFlow Computation Fluid Dynamics Software, Version 2.11.1, AEA Technology Engineering Software Ltd, 2001.